

# IMAGE ANALYSIS AND SEGMENTATION OF ANATOMICAL FEATURES OF CERVIX UTERI IN COLOR SPACE

Viara Van Raad

STI-Medical Systems, Honolulu, HI 96 813, USA  
e-mail: viarav@ieee.org

## ABSTRACT

We propose and verify a method for color-based cluster segmentation of the various tissues from ectocervix. That method uses a simplified compartment-like analysis, aiming for a Gaussian Mixture Model (GMM)-tailored segmentation. The tissues of interest are the cervical canal (CC), the columnar epithelium (CE), the squamous epithelium (SE) and the transformation zone (TZ) the latter known as area where pre-cancer is often found [1]. We used an optimization algorithm (maximum-*a priori* algorithm or MAP) for bimodal segmentation in normalized RGB color-space, as initially we estimated the deterministic values of CC, TZ, CE and SE as pixel sets in a compartmental-like mode. We assessed the MAP algorithm via automatic segmentation of squamous intraepithelial lesions (SIL) and CC. Our segmentation method is based on the estimates of the GMM boundaries for CC, TZ, and SE and their adjacent area-ratios for healthy ectocervices. We demonstrated a segmentation algorithm for CC and pre-cancer lesion detection that performed with high accuracy .

## 1. INTRODUCTION

Cervical cancer is the second most common cancer amongst women worldwide [2]. It is also the third most common cause of cancer-related deaths [3]. However, with early detection, cancer can be prevented and treated, so the risk of death is greatly reduced. Currently, in the clinics, there are two primary ways to find out if there is a pre-cancer on the cervix. One way is by taking a sample of cells from the surface of the woman's cervix and later performing a cytostest *in vitro*, known also as the Pap smear test. The other one is named colposcopy and it examines the cervix *in vivo* using broadband light and this can be done after positive Pap smear. Forming an overall diagnostic impression based on visual impressions cervical cancer precursors is a complex task. Experts consider factors such as color, texture and location of the shape of lesion(s), their borders for diagnosis. Accuracy in colposcopy for staging neoplasia varies among experts [4]. For these precursors to be diagnosed successfully, one has to understand and interpret these usual signs, introducing quantitative measures [5]. Extensive training is required for colposcopists to accurately evaluate if signs of cancer are present [1] onto ectocervix. The colposcopists' training is based on how the human visual system (HVS) perceives color, texture and shapes on the cervix. This is often too complex to be simulated by computer algorithms. In order to mimic the colposcopists performance automatically, our aim is

to find a simplified approach for automatically discriminating important anatomical features of the cervix by using quantitatively estimated values in a color-based segmentation task. Color-based classification and segmentation can provide an increased accuracy in computer aided diagnosis (CAD) and besides textural information of the appearance of vessels and other lesions, it uses the color intensity information from the image. We suggest a model that uses *a-priori* information based on assumed Gaussian Mixture Model (GMM) in color space in the current paper and in addition, we proposed a simplified compartmental-like modelling of region of interest (ROI), assessing the color space values against the complementary (ROI<sup>C</sup>). For a normal cervix, we defined at least four classes of image pixels to be analyzed, while for disease diagnosis there are more features and tissue types ([1] and [6]). The tissues of interest in a healthy cervix are the cervical canal (CC), the columnar epithelium (CE), the squamous epithelium (SE) and the Transformation Zone (TZ). The latter is known as area where pre-cancer is often found [1].

Previously, Pogue et al. evaluated the contribution of color-based analysis in digital colposcopic images[7]. However, they concluded that color analysis contributed only minimally to staging cervical intraepithelial neoplasias (CIN). Color-based segmentation and artefact correction using probability and *a-priori* estimates was proposed previously in [5]. In a similar probabilistic approach using "projection of convex set" (POCS) method, color was used for segmentation in [9].

The outline of this paper is as follows. Section 2 describes the estimation of parameters, that sets the scene for the MAP algorithm. Section 3 describes the theory behind MAP. Section 4 contains a detailed description of the bimodal approach used in the current experiments. Section 5 contains the experimental results for color-based segmentation, and Section 6 discusses the recommended method and concludes the article.

## 2. ESTIMATED PROBABILITY VALUES

Predominantly, the cervical landmarks in the colposcopy images are "nested" types of anatomical areas: the CC is placed centrally, often surrounded by the TZ. The latter is surrounded by the squamous epithelium (SE) [1]. We depicted the described spatial relationship in Figure 1, representing a stylized illustration of the spatial relationships between these areas in colposcopy images. The relative size of each anatomical feature appearing as a 2D projection on the image plane can be used for probabilistic modelling for *a-priori* estimation of the area

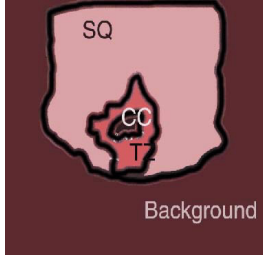


Figure 1: Stylized relationship of the 2D projection of a cervical image. The features are often “nested” one in another, which is a typical for endoscopy type of image.

occupied by each tissue type. The probability of that pixel that belongs to a type of tissue is proportional to the area after each tissue class occupies. That is why we established standard occupied relative areas of tissues as by measuring the ratio to the total image area of fifty healthy cervixes. It is possible that the area of the TZ or texture lesions might be indicative for the state of the health of the cervix. These measurements were performed via a semi-automatic (interactive) Matlab-based program, which asks a trained operator to delineate the outer polygons associated with each tissue class. The fact that the polygon areas are nested, makes the inner boundary of the surrounding tissue also the outer boundary of the inner tissue type. The sample average of the area (the mean), the variance and the area occupied by the tissues were calculated using the Green’s lemma for area on a discrete grid. The measurement was performed using the simplified model of CC, TZ and SE displayed on Figure 1. The portion of the area occupied by the CC, TZ, SE and SR are as follows: CC occupies about **2%** or less of the 2D projection of the ecto-cervical area; TZ occupies approximately **28%** or less from the full area of the normal cervix; SE occupies around **70%** or less from the normal cervix. The results represent the pooled average values taken from the training set, selected out of fifty normal cervixes. More test pixels were taken from the smaller area regions, approximately proportional to the area of the feature.

### 3. MAP THEORETICAL BACKGROUND

The digitized color cervical images are a 2D projection (onto image plane) of the cervix, represented as RGB triplets. Segmentation based on RGB triplets (3-tuples) is difficult because of large variation in color among the same type of tissue represented on color image (as an example SE) in healthy cervixes. This was illustrated on Figure 2. Assuming that the data has normally distributed probability density function (pdf), each of the data sets under investigation is represented by a set-variable  $S_Z$ , where  $Z$  describes separate random processes. Let  $\mathbf{z}$  is a vector of the corresponding random variable with 3-tuple values for the three-color components, that interchangeably belongs to each of the tissue types, such as the CC, the TZ, the SE and the artifact named specular reflection (SR). Our experimental study is based on large pixel samples. The number of samples  $\hat{N}$  for training data for each tissue type lies within the range

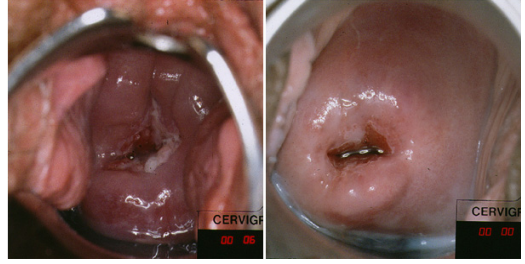


Figure 2: Variation of the color of the normal SE in two healthy cervixes.

of  $2.5E + 6 - 10E + 6$  pixels for each of the experiments for empirical assessment of the multiple component pdf(s). The sample size was selected to be proportional to the probability of occurrence of each of the  $S_{Z=CC|TZ|SE|SR}$ . The GMM of  $D$ -dimensional multivariate distribution  $\lambda$  can be parameterized as:

$$P(\underline{x}|\lambda) = \sum_{j=1}^D w_j \frac{1}{(2\pi)^{D/2} |\underline{\Sigma}_j|^{1/2}} \times \dots \exp^{-\frac{1}{2}(\underline{x}_j - \underline{\mu}_j)' \underline{\Sigma}_j^{-1} (\underline{x}_j - \underline{\mu}_j)}, \quad (1)$$

where  $w_j$  are the component mixture weights;  $\underline{x}_j$  and  $\underline{\mu}_j$  are vectors of  $\hat{n}$ -tuple values from the  $j^{th}$  color class, as the latter is the estimated pooled mean from the training image set. The former are the  $\hat{n}$ -tuple test vector of pixels under classification.  $\underline{\Sigma}_j$  is the covariance matrix of  $j^{th}$  and  $|\underline{\Sigma}_j|$  is the determinant of the covariance matrix  $\underline{\Sigma}_j$ . The joint likelihood of the independent and identically distributed (i.i.d) feature vector observations may be specified as a product of each one of the modelled probability:

$$P(\underline{x}|\lambda) = \prod_{j=1}^D p(\underline{x}_j|\lambda), \quad (2)$$

which in logarithmic terms is the corresponding sum:

$$\underline{\mathcal{L}}(\lambda) = \sum_{j=1}^D \ln p(\underline{x}_j|\lambda). \quad (3)$$

Thus we can model each of the  $D$  - elements of the mixture in color space and we can determine the  $\hat{n}_{(\hat{n}=3)}$ -tuple RGB cluster boundaries of the normally distributed data with mean and covariance. The set of pixels  $Y = \{y_1, y_2, \dots, y_n\}$  on a colposcopy image ( $n$  is the number of pixels in the image) is assumed to belong to a random process  $X = \{x_1, x_2, \dots, x_n\}$ , where an underlying segmentation is fulfilling the simple model:

$$x_J \in \underline{\mathcal{L}} = \{1, 2, \dots, D\} \quad (4)$$

$\underline{x}_j = \mathbf{z}$  and  $Z$  is the underlying and “sought” random process. This will indicate that the pixel  $i$  belongs to



Figure 3: A stylized image (the far left image) and the four compartments-like description of the four classes for CC, TZ, SE and Background.

tissue type  $\mathbf{z}$ . We define the probability that pixel belongs to a tissue of type  $z$  by the non-negative quantity  $\rho_j^z$ , so  $P(x_j = \mathbf{z}) = \rho_j^z$ , which also is the probability for the set of pixels representing a random process  $Z$  and it can be expressed as  $P_Z(z)$ . We know that:

$$\sum_{j=1}^D \rho_j^z = 1. \quad (5)$$

The observed image model is  $X$ , while ideally *the most probable selection of pixel sets* in the image  $Z_{MAP}$  is to arise (to be discovered). The latter is in some sense the ideally sought image segmentation, given “a-priori” knowledge about the observation process  $X$ . This is known as the MAP approach, while the Maximum likelihood estimate (ML) is to estimate  $\mathbf{z}$  (a vector) with the image  $z_{ML}$  which maximizes the likelihood that our observation will occur. This is:

$$Z_{ML} = \arg \max_{\mathbf{z}} P_{X|Z}(\mathbf{x}, \mathbf{z}) \quad (6)$$

The formula for the MAP in that case is:

$$Z_{MAP} = \arg \max_{\mathbf{z}} P_{Z|X}(\mathbf{x}, \mathbf{z}), \quad (7)$$

that’s using the Bayesian rule, the relationship between ML and MAP is:

$$P_{Z|X}(\mathbf{z}, \mathbf{x}) = \frac{P_{Z|X}(\mathbf{x}, \mathbf{z})}{P_X(\mathbf{x})} = P_{X|Z}(\mathbf{x}, \mathbf{z}) \frac{P_Z(\mathbf{z})}{P_X(\mathbf{x})}. \quad (8)$$

As an emerging random process, that leads to the occurrence of  $\mathbf{z}$ , we can estimate the approximation of  $P_Z(\mathbf{z})$  deterministically using MAP method (for example, using the estimates for the ratios of the areas occupied form the training set for CC, TZ, SE and SR). We are suggesting even more simplified model (Figure 3). We consider that we can estimate empirically the bounds for these tissue types (as pixel values) by using the 50 training images. Each time we are assuming bimodal distribution - e.g. a “foreground” and a complementary “background,” for which the foreground is  $S_Z$  and the “background” is  $S_Z^C$  (Figure 3). In that way, *we will be not interested in the latter estimate*, but the estimates of  $S_Z^C$  are included for the calculations in the MAP algorithm. Our focus is on establishment of the empirical values of the pixels that belong to  $S_Z$ . The collected information can be used for MAP segmentation as in equations 7 and 8 for  $P_Z(\mathbf{z})$  with pooled values for CC as  $S_C$ ; TZ as  $S_{TZ}$ ; SE as  $S_{SE}$ ; and SR as  $S_{SR}$ .

Thus we will be determining the bounds of  $\mathcal{N}(\underline{\mu}_Z, \underline{\Sigma}_Z)$  in color space using the absolute pixel intensities ( $R, G, B$ ) or their chromaticity, as the latter are less-illumination dependent.

#### 4. THE MAP ALGORITHM FOR SEGMENTATION

The tissue class set  $Z$  can be modelled as if it belongs to a bivariate GMM. The two-feature vectors ( $S_Z$  and its complimentary  $S_Z^C$ ) are assumed as set-variables members of a bivariate distribution that consists of “foreground” and “background” (Figure 3). The joint likelihood of the i.i.d vectors’ observations as product of these probabilities will yield:

$$P(\underline{x}|\lambda) = p(\underline{x}_Z|\lambda)p(\underline{x}_Z^C|\lambda), \quad (9)$$

as this equation is a partial case of equation 2 for the bimodal case, which yields the equation 9. The latter causes the selected modelled process  $\mathbf{z}$  to be tested out in order to maximize the chances of the pixel under test to belong to particular class. This, according MAP’s theory is to be judged by the logarithmic distance  $\Delta_Z$  between the clusters (equation 10), in order to find the sought pixel set. The distance is:

$$\Delta_Z = 2 \ln \left[ \frac{\rho_Z |\underline{\Sigma}_Z|^{1/2}}{(1 - \rho_Z) |\underline{\Sigma}_Z^C|^{1/2}} \right] \quad (10)$$

Thus, the following inequality (equation 10) states the criteria for the  $\hat{n}$ -tuple variable  $\underline{x}_j$ . The inequity is a mathematical derivation from the logarithmic expression in equation 3 for the bimodal case (equation 11):

$$\underline{\mathcal{L}}(\lambda) = \ln p(\underline{x}_Z|\lambda) + \ln p(\underline{x}_Z^C|\lambda). \quad (11)$$

The inequality that represents the criteria if a selected vector is chosen to belong to  $Z_{MAP}$ :

$$\mathbf{x}_i \in S_{Z_{MAP}} \text{ if } \begin{cases} (\mathbf{x}_i - \underline{\mu}_Z)' \underline{\Sigma}_Z^{-1} (\mathbf{x}_i - \underline{\mu}_Z) - \\ - (\mathbf{x}_i - \underline{\mu}_Z^C)' \underline{\Sigma}_Z^{C-1} (\mathbf{x}_i - \underline{\mu}_Z^C) \leq \Delta_Z, \\ \text{otherwise } \mathbf{x}_i \in S_Z^C \end{cases}, \quad (12)$$

where  $\underline{\mu}_Z$  and  $\underline{\Sigma}_Z^{-1}$  are the mean vector and covariance matrix of the 3-tuples for the pixels that belong to the  $S_Z$ . The  $\underline{\mu}_Z^C$  and  $\underline{\Sigma}_Z^{C-1}$  are the deterministic values from the training image for the pixels that belong to  $S_Z^C$ .

#### 5. EXPERIMENTAL RESULTS

MAP-based experiments for detection and correction of an artifact in cervical images known as glare or specular reflection (SR) were presented previously in [8]. Another attempt to remove the glare was the “ad-hoc” method described in [10]. In this research, we used the MAP approach, testing the ability of our bimodal model to achieve an automated differentiation of the pixel set  $S_{CC}$  (the cervical canal) from the rest of the image  $S_{CC}^C$ , which was based on the equations (10) and

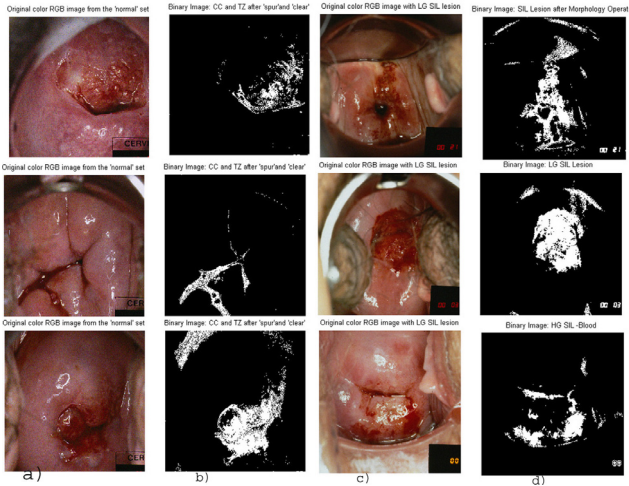


Figure 4: a) Each of the 3 color RGB images on the left is from healthy woman. b) Illustration of segmented cervical canal (CC) binary images c) Each of the 3 color RGB images has a lesion. d) Segmented CIN I SIL lesions as binary images of the right. The image is segmented by previously described MAP algorithm for  $S_{CC}$  and  $S_{CC}^C$  differentiation. This algorithm “detects” lesions that have “bloody” appearance.

(12) for twenty five images. Thus we calculated if a pixel belongs to that set, using a probability based distance measure, described before as the *mean* and the *adjacent covariance*  $\{\hat{\mu}_{CC}^C; \hat{\Sigma}_{CC}^C\} \in S_{CC}^C$  in chromaticity or *rgb* space. Thus, the local chromaticity for pixel  $y_i$  or the local illumination independent chromaticity value is:  $\{\frac{y_{iR}}{y_{iR}+y_{iG}+y_{iB}}, \frac{y_{iG}}{y_{iR}+y_{iG}+y_{iB}}, \frac{y_{iB}}{y_{iR}+y_{iG}+y_{iB}}\}$ . The values are 3-tuples. We achieved fully automatic CC segmentation shown on Figure 4 b) and lesion segmentation from the images with pre-cancer in the third column. The accuracy of the segmented area for the normal group of selected test images (Figure 4 b)) was 95%, which was evaluated by the method for comparison of the ground truth from the pre-defined masks. The accuracy of the segmented area from the pre-cancerous test images was 86% successful accuracy, evaluated by the same method. This verification method uses pre-annotated masks that defines “target” based on colposcopy impressions only.

## 6. DISCUSSION AND CONCLUSIONS

We studied the GMM based MAP probability model in cervical images in color space. This probabilistic approach was novel to cervical image analysis, considered the specific application. The suggested method is a general statistical method that can be applied to many other problems such as machine vision and pattern recognition. It has shown success in other applications, it is simple to implement, and it can be implemented in algorithm that is easy to follow. On the other hand, there is a disadvantage of this method because the method *is not an adaptive method* and in the “training” phase it uses device-specific color-based values. The method can be improved if the colposcopy

images are pre-calibrated. The method can be used in color-based image analysis if a detail annotations are available within the training set.

**Acknowledgements:** The work presented in this paper was funded by the School of Electrical Engineering and Telecommunications, University of New South Wales, Kensington and the Australian Research Council (ARC<sup>1</sup>). This paper was motivated by Prof. B. Celler and A. Prof. H. Outhred, for which I am thankful. I appreciate the suggestions and comments regarding the contents, structure and style of the article, made by Gary Bignami (Science and Technology International).

## REFERENCES

- [1] Campion M. J. , Ferris D. G., di Paola F. M., “Modern Colposcopy,” Educational Systems, Inc. Augusta, Georgia, USA 1991.
- [2] American Cancer Society. Cancer Facts and figures 2003. Atlanta (GA):ACS; 2003. database (<http://www.cancer.org/downloads/STT/CAFF2003PWSecured.pdf>).
- [3] Sawaya G.F., Brown A.D., Washington A. E. Garber A.M., “Clinical Practice. Current Approaches to cervical cancer screening,” N.Eng. J. Med. Vol. 344(21), pp.1603-1607, 2001.
- [4] Massad L. S. and Collins Y. C., “Strength of Correlations Between Colposcopic Impressions and Biopsy Histology,” Gynecol. Oncol., Vol. 89, pp. 424-428, 2003.
- [5] Viara Van Raad and Andrew Bradley, “Emerging Technologies, Signal Processing and Statistical Methods for Screening of Cervical Cancer in vivo - Are they good candidates for Cervical Screening?,” IEEE - IEE Proc. of Advances in Medical Signal and Inf. Processing, Vol. 2, pp. 210-217, 2004.
- [6] Apgar, B. S., M. M. Rubin, et al, “Ch. 5: Principles and technique of the colposcopic examination. Colposcopy: Principles and Practice.” B. S. Apgar, G. L. Brotzman and M. Spitzer. Philadelphia, W.B. Saunders Company, pp. 115-146, 2002.
- [7] Pogue B. W. , Mycek Marry-Ann, D. Harper, “Image Analysis for Discrimination of Cervical Neoplasia,” J. BioMed. Optics, Vol. 5(1), pp. 72-82, 2000.
- [8] Van Raad V. , “Frequency Space Analysis of Cervical Images using Short Time Fourier Transform,” Proc. of IASTED, Intern. Conf. of BioMed Eng., Vol (1), pp. 77-81, 2003.
- [9] Gordon S., Zimmerman G., and Greenspan H., “Image segmentation of Uterine Cervix images for indexing in PACS,” Proceedings of the 17th IEEE Symposium on Computer-Based Medical Systems (CBMS’04), 2004.
- [10] Lange H., “Automatic Glare Removal in Reflectance Imagery of the Uterine Cervix,” to appear in SPIE Proc. 5747, Medical Imaging, San Diego, Feb. 12-17, 2005, *in press*.

<sup>1</sup>ARC-Strategic Partnership with Industry – Research and Training (SPRIT), Project ID: C0001944, 2000-2004.